AIRISC -A mmWave Angle-Insensitive Reconfigurable Intelligent Surface Communication System

Carola Rizza, Valeria Loscri

AIRISC - A mmWave Angle-Insensitive Reconfigurable Intelligent Surface Communication System

Carola Rizza
Inria Lille, France
carola.rizza@inria.fr

Valeria Loscri
Inria Lille, France
valeria.loscri@inria.fr

Abstract

This paper presents a Reconfigurable Intelligent Metasurface (RIM) with beam-steering capabilities working in the millimeter frequencies and being insensitive, namely supporting a wide range of angles of incidence, up to 75°. Particle Swarm Optimization (PSO) algorithm is adopted to reconfigure the metasurface according to the desired direction of the reflected main beam. Finally, the interference has been modeled and a system model including a base station, a RIM and a mobile receiver, in presence of interference is considered, and the performances of the system are evaluated through the angle deviations of the obtained main beam, the change of the sidelobe level (SLL) and the accuracy.

Keywords

Interferers, beam-steering, metasurface, mmWave, PSO.

1 Introduction

During the last years there has been a growing interest on Reconfigurable Intelligent Metasurfaces (RIMs). Metasurfaces are surfaces made of electromagnetic material that are engineered in order to exhibit properties that cannot be found in naturally occurring materials. RIMs include also phase switching components that allow to reconfigure the behaviour of the metasurface to adapt itself to the changing requirements of the surrounding environment. In this way, they can manipulate electromagnetic waves in unconventional ways, overcoming Snell's law constraints. Functionalities like beam steering and focusing, wave absorption, polarization changing and phase control can be realized.
The environment including such metasurfaces is turned into a software-reconfigurable entity, that can be optimized to enable uninterrupted connectivity and guarantee quality of service.
Metasurfaces show also other attractive features, including ultrathin thickness, low loss, easy fabrication, and low cost [1],[2] and [3].
Most of the metasurfaces found in literature are designed for orthogonal incident angles, but as it is possible to notice from [4] and [5], the behaviour of the metasurface depends on the angle of incidence, that can be different than the orthogonal one. For this reason, for real environments it would be better designing metasurfaces insensitive to the angle of incidence [6], [7].
The tremendous increase of traffic demands requires to move to higher frequencies, i.e. millimeter wave and THz, where there is great availability of unused frequency bands. Besides, these frequencies allow to reach very high data rates and device size miniaturization [8],[9].

In literature there are some meta-atom structures designed to perform beam-steering. In [10] and [12], the authors propose a unit-cell that can perform beam steering but both are designed to work in the microwaves. [11] presents a meta-atom that is adopted for a metasurface that is able to perform beam deflection, multi-beam and beam diffusion, but it works around 7 GHz and it results "insensitive" to angles up to 30°. These meta-atoms have not been designed to work with a wide range of angles of incidence. [23] proposes a 3-bit RIS meta-atom operating at large angles of incidence, between 0° and 60°, but this structure has been designed to work at around 3 GHz, so outside the millimeter range. Also [24] presents a programmable meta-atom structure, insensitive to the angle of incidence up to 60° , but working outside the considered frequency range considered in this work.
This work presents a novel reconfigurable intelligent metasurface able to perform beam-steering in mmWave frequencies. It has the advantage to be insensitive to the angle of incidence up to 75°. The control of the direction of beams generated by the metasurface towards a target receiver, is realized by the means of a Particle Swarm Optimization (PSO) algorithm. Finally, our metasurface is placed inside a system including a base station and a mobile receiver and the impact of the interferers on the ability of the metasurface of tracking the user is evaluated.

The contributions of this paper can be summarized as follows:

- A new RIM working in the mmWave is presented. It has the peculiarity to be insensitive to the angle of incidence up to 75°;
- A PSO algorithm has been adopted in order to control the phase configuration of the metasurface for beam steering purposes;
- Interference is considered and modeled in the system and more specifically, a configuration with a base station, our RIM and a mobile user in presence of scatterers is presented;
- The performances of the communication system have been evaluated in presence of a different number of scatterers.

This paper is organized as follows. In Section II the related work is presented. The structure of designed meta-atom is explained in Section III. In Section IV the behaviour of the presented meta-atom is discussed in terms of scattering parameters. Section V presents the adoption of PSO algorithm in order to find the required phase configuration of the metasurface. The system model based on a transmitter, reconfigurable intelligent metasurface and receiver is presented in Section VI in presence of interference. Section VII discusses the performances of the considered system. In Section VIII, we discuss the performance of the RIM-based system in a pedestrian tracking scenario. Finally, the paper ends with conclusions in Section IX.

2 Related Work

In this section we consider three main related contributions in the literature. The first one is concerning the metasurfaces whose working frequency is in mmWave. The other works are related to the insensitive metasurfaces contributions. Finally, the interference models are presented.

- mmWave Beamsteering Metasurfaces:
In literature there are some meta-atom structures designed to perform beam-steering in mmWave. In [16], the authors make reconfigurable metasurfaces capable of deflecting electromagnetic waves in an electronically controllable fashion. This is obtained by embedding inside metasurface unit-cells electronically-controlled phase-change materials. This metasurface can perform beam-steering at $100GHz$, offering up to 44° beam deflection in both horizontal and vertical directions. [17] presents voltage-controlled millimeter-wave beam-scanning through a fully-integrated vanadium dioxide reconfigurable meta-surface. It is demonstrated that the millimeter-wave beam direction is scanned electronically by applying appropriate voltages across the array, and achieve 44° of beam-scanning at 0.1 THz. In [18], the authors present a fully-integrated and electronically-controlled millimeter-wave beam-scanner based on a reconfigurable meta-surface. 44° of continuous beam-scanning are demonstrated at 95 GHz. [19] presents a low loss metamaterial unit cell with an integrated GaAs air-bridged Schottky diode to produce a dynamically tunable reflective phase shifter that is capable of up to 250° phase shift. It is shown that this diode-based unit cell can be integrated into metamaterial components, which have potential applications in future mmWave antenna beam-steering. [20] proposes a single-beam prephased 1 bit reflective metasurface to achieve single-beam patterns under normally incident plane waves. It has the potential to achieve beamforming and beam scanning for mmWave indoor communications. In [21], the authors introduce a wall-mounted smart metasurface, called mmWall, that enables a fast mmWave beam relay through the wall and redirects the beam power to another direction when a human body blocks a line-of-sight path. Moreover, the mmWall supports multiple users and fast beam alignment by generating multi-armed beams. [22] introduces a low-cost and reconfigurable metasurface placed in the environment to reshape and resteer mmWave beams. By encoding the phase shifting values, the metasurface can reshape and resteer mmWave beams, thus enabling a fast mmWave beam relay through the wall, or redirects the beam power to another direction when a human body blocks the LOS path.

- Insensitive Metasurfaces As regards the insensitivity to the angle of incidence, it is difficult to find metasurfaces. [23] proposes a 3-bit RIS meta-atom operating at large angles of incidence, between 0° and 60°. But this structure has been designed to work at around 3 GHz, so outside the millimeter range. Also [24] presents a programmable meta-atom structure insensitive to the angle of incidence up to 60° but working outside the considered frequency range in this work.

- Incidence Angle Insensitivity In the following, papers on interference models with metasurfaces found in literature are presented. In [25], path loss models for RIS-assisted wireless communications are developed, but the authors only consider ideal links in line-of-sight between the transmitter/receiver and the RIM. [26] includes mmWave channel models and massive MIMO architectures but it does not take into account the effect of the RIM over the channel. [27] does an overview of the channel models that include reconfigurable intelligent metasurfaces. In [28] a two-path propagation model is proposed for RIS-assisted wireless networks by considering both the direct path from the transmitter to the receiver and the assisted path established by the RIS. Phase shifts of RISs are optimized by appropriate configuration for multipath fading mitigation. In [29], authors capitalized on the 5G mmWave channel model with random number of clusters/scatterers and extended it to include an RIS. The proposed model is valid for RIS-empowered narrowband communications in indoor and outdoor environments and includes many physical characteristics, such as LOS probability, shadowing effects, and shared clusters. In addition, the model incorporates realistic gains and array responses for RIS elements in addition to the existing channel models. [30] proposed an indoor wireless communica-

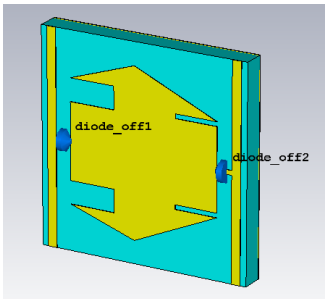

Figure 1. 4-state meta-atom with both diodes in off state.

tion paradigm where the electromagnetic propagation environment becomes aware of the ongoing communications within it, since HyperSurface tiles are adopted to cover obstacles. [31] proposes a three-dimensional (3D) communication channel model for an indoor environment considering the effect of the Hypersurface (computer-controlled active metasurface) on the 60 GHz mmWave frequency band. The Hypersurface can control the impinging rays from a transmitter towards a receiver location in both LOS and NLOS paths. [32] presents a channel model with reconfigurable intelligent surfaces (RISs) in the mmWave band. Gain properties of the RISs in LOS channels are analysed with respect to frequency and size. In respect of the mentioned contributions, we propose a full analysis of a metasurface working at mmWave, insensitive up to 75° and in presence of interference. To the best of our knowledge, the behavior analysis of an insensitive metasurface in presence of interference has not been yet considered in current literature.

A previous work related to this article is [33]. In this article an improved version of the metasurface to be insensitive to the angle of incidence is adopted. The effect of the interferers on a realistic outdoor wireless system including the angle-insensitive metasurface is evaluated. Moreover, performances of a system where the designed metasurface is adopted to track a mobile receiver at different speeds are evaluated. Anyway, in [33], the proposed metasurface is insensitive up to 30° and the optimization algorithm was based on a genetic approach.

3 Meta-atom design

In this section, the designed meta-atom structure is presented. It consists of a metallic pattern with an irregular shape, over a dielectric substrate and a ground plane, as shown in Fig. 1. In the metallic pattern, there are two diodes that, together with a via hole placed on the right part of the metallic pattern, make the structure reconfigurable in terms of phase. The via hole connects the metallic pattern upon the substrate to the ground plane.

The substrate is made of F4B, whose dielectric constant is 2.65 and the electric tangent loss is 0.001. It has a square shape with each side of length 3.81 mm and its thickness is 0.41 mm. The pattern upon the substrate is

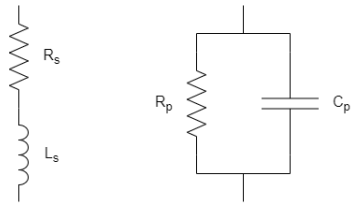

Figure 2. Equivalent circuit of the adopted diode.

Table 1. Value of the PIN diode equivalent circuit elements

Component	value
R_s	4.2 Ω
L_s	0.1nH
R_p	60kΩ
C_p	23fF

made of copper and it has been designed starting from two rectangles of different dimensions with two right-angled triangles of different dimension on both the upper and the lower side. On the obtained structure, 4 cuts have been performed. The via hole has a radius of 0.16 mm. The diodes have been modeled as shown in Fig.2 [34]. The values of the equivalent circuit components are shown in Table 1. It is worth to highlight that the adoption of a real diode, instead of an ideal diode, makes easier the prototyping of the metasurface and account for realistic behaviour of the meta-atom in respect of the beam-steering capacity of the system. In the y direction two biasing lines have been added in preparation for the entire metasurface made of the repetition of many identical unit-cells, where only the state of the diodes can be modified. This unit-cell has been designed by adopting the conventional approach of "trial and error". This approach is recognized to give the possibility to explore a large space of solutions, even though it is time and computational consuming. Only recently, research efforts have started to focus on deep learning approaches to improves the design of metasurfaces with specific features as shown in [35] and [36]. Anyway, since in this work we are interested to a specific functionality for reconfigurable intelligent metasurfaces, namely beam steering, the "trial and error" approach has been considered suitable for the design of our meta-atom. During the design of the meta-atom through the aforementioned approach, we have taken into account that the metasurface works in the mmWave frequencies, that it is able to generate the required radiation patterns in order to do beam-steering and that the meta-atom has four possible states in order to have enough control on the behaviour of the metasurface. Moreover we have tried to minimize the number of pin-diodes in the structure in order to reduce the costs of the metasurface.

4 Evaluation of the meta-atom features

In this section the behaviour of the designed meta-atom is presented. In order to have a metasurface that can perform beam-steering, the unit-cell should be fully

reflective and the phases of the reflection coefficient should be shifted of an amount equal to around 90° when the state of the meta-atom is changed.
The meta-atom has been simulated on CST (Computer Simulation Technology [37]). According to the chosen settings ("unit cell" boundary in x and y directions and "open add space" in the other one), an infinite structure based on the repetition of the meta-atom has been simulated. These settings have established also the illumination of the structure. *Floquet ports* have been created that allow to generate plane waves. The number of excited modes has been set to two, corresponding to the two fundamental modes, TE(0,0) and TM(0,0), that are linearly polarized plane waves. However, the results shown in the section refer only to TM(0,0) mode. For convenience, it has been chosen that the plane wave incides orthogonally to the meta-atom.

The scattering parameters have been computed for all the states of the diode. In particular, the reflection coefficient S_{11} has been taken in greater account. Indeed, in order to build metasurfaces able to perform beam steering, it is required that the unit-cell maximizes the reflected signal. This is translated in having a reflection coefficient almost equal to 0 dB in the frequency range of interest. The obtained reflection coefficients, in modulus, are shown in Fig. 3.

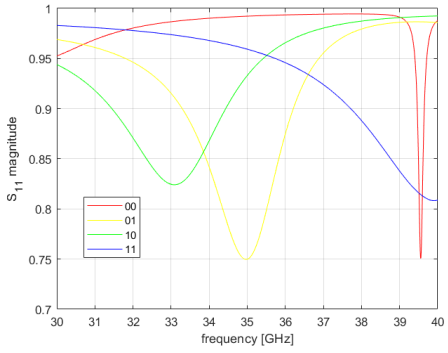

Figure 3. Reflection coefficient S_{11} in modulus of the meta-atom of Fig. 1 for all the four configurations of the diodes.

For all the states of the meta-atom, S_{11} is quite closed to 1: the lowest value is 0.8 and occurs for the state '01'. In order to design a metasurface which can steer the direction of the reflected signal in a wide angular range, the *generalized Snell's law of reflection* is adopted. This method consists in searching the required surface phase profile of the metasurface in order to transform the incident wave with direction θ_i in a reflected wave with direction θ_r by tailoring the surface impedance. The desired field distribution of the reflected wave from the metasurface are:

$$H_r = H_r e^{-jk(sin(\theta_r)y+cos(\theta_r)z)}x \tag{1}$$

$$E_r = \eta H_r(sin(\theta_r)z - cos(\theta_r)y)e^{-jk(sin(\theta_r)y+cos(\theta_r)z)} \tag{2}$$

since we have considered TM mode.
The total electric field at the surface is written as:

$$E_t = \mathbf{E_i}e^{-jksin(\theta_i)y} + \mathbf{E_r}e^{-jksin(\theta_r)y+j\phi_r} \tag{3}$$

From this formula, the desired phase of the reflection coefficient is:

$$\Phi_r(y) = < \left(\frac{\mathbf{E_r}e^{-jksin(\theta_r)y+j\phi_r}}{\mathbf{E_i}e^{-jksin(\theta_i)y}}\right) = -ksin(\theta_r)y + \phi_r + ksin(\theta_i)y \tag{4}$$

As it is possible to notice from this formula, the phase has a sawtooth behaviour with respect to the direction y and their values vary from -180°to 180°. By differentiating this formula with respect to y, the gradient of the reflection coefficient in the generalized Snell's law is obtained [13]:

$$\frac{d\Phi_r(y)}{dy} = k(sin(\theta_i) - sin(\theta_r)) \tag{5}$$

that gives a relationship between the angle of incidence θ_i, the angle of reflection θ_r and the local surface phase $\Phi_r(y)$. When θ_r is very close to θ_i, the phase profile varies slowly through the surface.
In our case θ_i=0°, so the phase profile depends only on the reflection angle.
Since the metasurface consists of many sub-wavelength sized elements, the desired local phase shift is approximated by assigning a constant phase shift to each meta-atom. The smaller the elements are, the better the local phase shift can be approximated. Dividing the metasurface in many unit-cells has no effect on the magnitude of the scattered field and on the beamwidth. The electric field of the incoming electromagnetic wave induces a surface current of the direction of the field. By tuning the surface impedance of each element, the current is adjusted and, thus, the reflected field in the desired direction θ_r is resulted.
Since a 4-state meta-atom has been chosen for this application, four discrete possible values of the phase can be adopted that are equispaced of about 90°. The phase of the reflection coefficients of the four states of the meta-atoms is shown in Fig. 4.

As it is possible to notice from the graph, the reflection coefficients of the four configurations are shifted of around 90°at frequency f=34.35 GHz, that is the working frequency of our system.

The behaviour of the meta-atom has been evaluated also for other angles of incidence. As it is possible to notice from the graphs, about 90°phase shift is maintained until ± 75°of incidence. The corresponding values of the angles for the different incidence angles are reported in Table 2.

Table 2. Scattering parameters

		0°	15°	30°	45°	60°	75°	88°
00	mod	0.99	0.99	0.99	0.99	0.99	0.98	0.9
00	phase	26.8°	30.32°	46.32°	69.56°	101.32°	140.3°	-135.82°
01	mod	0.8	0.8	0.8	0.81	0.82	0.86	0.98
01	phase	-124.6°	-123.16°	-105.25 °	-81.55 °	-52.84°	-16°	-1.97°
10	mod	0.89	0.9	0.95	0.92	0.92	0.92	0.97
10	phase	98.79°	93.61°	98.85 °	132.7°	164.51°	-135.48°	-24.22°
11	mod	0.96	0.97	0.97	0.97	0.97	0.96	0.99
11	phase	-46.62°	-46.58°	-25.4°	1.13 °	32.08 °	48.97°	10.81°

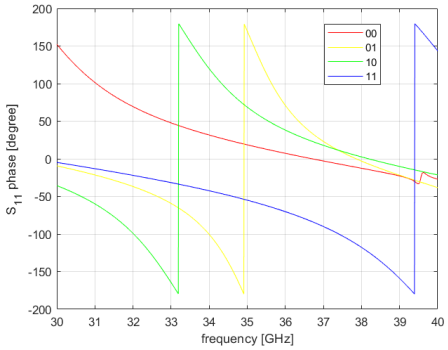

Figure 4. Phase of the reflection coefficient S_{11} of the meta-atom of Fig. 1 for all the four configurations of the diodes.

5 Computation of the phase configuration based on Particle Swarm Optimization

In order to find the phase configuration of the metasurface that generates the desired radiation pattern, a Particle Swarm Optimization (PSO) approach, has been adopted. The computation of the phase configuration can be expressed as an optimization problem, in which the objective function is the minimization of the difference between the computed radiation pattern and the desired one. So given the required radiation pattern, optimization algorithms PSO can be adopted to compute the correspondent coding matrix. The PSO algorithm is a metaheuristic algorithm based on the concept of swarm intelligence (SI) that was inspired by the movements of flocks of birds and of school of fish [38]. Systems like these consist of agents interacting locally each other and with the environment. Each agent is free to behave as it wants with a certain degree of freedom. Its behaviour, indeed, is affected by its personal experience and by the one of the other members [40].
In this algorithm, particles roam across the solution space from one iteration to the next one. In order to find the optimal solution, each particle moves towards the position of its previous best solution (pbest) and, at the same time, towards the global best solution (gbest).

$$pbest(i,t) = arg \min_{k=1,\dots,t} [g(x_i(k)], \qquad i \in \{1,2,\dots,N\} \tag{6}$$

$$gbest(t) = \underset{\substack{i=1,2,\dots,N \\ k=1,\dots,t}}{arg\,min}\, [g(x_i(k)] \tag{7}$$

where i is the particle index, t represents the current iteration, N is the total number of particle, g is the fitness function and x is the particle position. In this version of the algorithm, the particle position corresponds to the coding matrix of the metasurface. So *pbest* corresponds to the previous best configuration of a given particle and *gbest* corresponds to the global best configuration.
The velocity of the particles is computed as follows:

$$v^i_{k+1} = c_0 v^i_k + c_1 \eta_1 (\hat{x}_p - x_k) + c_2 \eta_2 (\hat{x}_g - x_k) \tag{8}$$

where c_0 represents the inertia weight and balances the global search ("exploration") and the local search ("exploitation"), while c_1 and c_2 are called "acceleration coefficients" and say how much the particle is affected by the global $\hat{x_g}$ and local best $\hat{x_p}$. η_1 and η_2 are two uniformly distributed variables within the range [0,1] and allow to avoid premature convergences. This formula consists of three terms. The first one is called "inertia" and represents the contribution given by the previous velocity v^i_k. If c_0=1, the new velocity is fully affected by the previous one; if it is lower, the particle can explore other regions of the search space, thus increasing the possibility to find a global optimum (but increasing also the simulation time). The second term is known as the "cognitive" component and represents the individual thinking of each particle. If the particle is far away from its local best $\hat{x_p}$, this term increases, thus attracting the particle towards $\hat{x_p}$. The parameter c_1 is a positive constant and weights the importance of the individual previous experience of the particle. The last part is named as the "cooperation" component because it represents the collaborative effect of all the particles to reach the global best solution. The difference $\hat{x_g}$ - x_k attracts the particles to the global best solution $\hat{x_g}$ and it is weighted by the parameter c_2 [40],[41].
As regards the particle position, it is updated according the following formula:

$$x^i_{k+1} = x^i_k + v^i_{k+1} \tag{9}$$

The new position of the particle depends on the previous position x^i_k and on the new velocity v^i_{k+1}.
PSO algorithm has been adopted to find the phase configuration of the meta-atoms that provides the wanted radiation pattern.

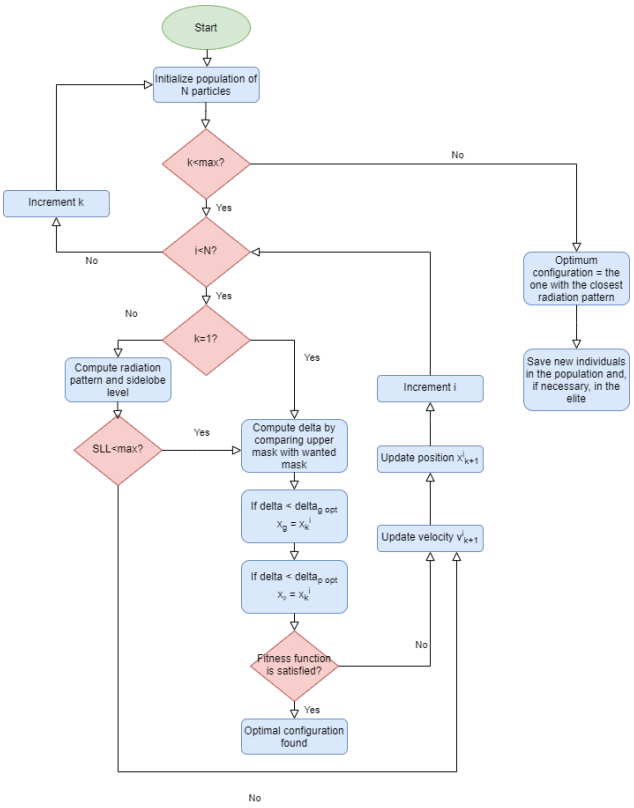

Figure 5. Flow-chart of the adopted Particle Swarm Optimization algorithm.

In input to the algorithm there is the wanted direction of the main beam in terms of elevation θ and azimuth ϕ angles and the acceptable level of the sidelobes (SLL $<$ 0.5). The PSO algorithm starts with the initialization of the particles, with their positions that correspond to the coding matrices, the radiation pattern that they generate and the θ and ϕ angles that characterize the main beam direction. The global best "position" among the ones of all the particles is set as the particle whose coding matrix gives the lowest delta (difference among the main beam angle and the required main beam direction) and the global best delta are updated. If the i-th particle shows a lower delta than the ones observed during all the previous iterations of the i-th particle, the local best "position" and the local best delta are updated. If the global best "position" gives a main beam with similar angles (with fixed tolerances ϵ_ϕ and ϵ_θ), the optimal solution if found. Otherwise, the new positions of the particles are computed according to their previous positions and their new velocities. The new velocities are computed from the previous velocities and from the distance of the local best position and the previous position of the particle and from the distance of the global best position and the previous position of the particle. Since the positions of the particles correspond to coding matrices made of 0, $\pi/2$, π and $3/4\pi$, the computation of the new positions of the particles is adapted in order to produce vectors of these values exclusively. If the new position of a particle provides lower delta wrt. the global best delta, the global best "position" is updated together with the global best delta. New positions of the particles are generated until the global best delta satisfies the conditions on the main beam direction or the maximum number of iterations is reached. The flowchart of the algorithm is shown in Fig. 5.

6 System Model

As shown in fig. 6, we consider a wireless system consisting of a transmitter, a RIM and a mobile receiver. Transmitter and RIM are at the same height and they are aligned in order to have the angle of incidence of the signal impinging on the metasurface equal to 0°. Scatterers are considered in the channel between transmitter and metasurface. They are grouped into C clusters, each one with S sub-rays which have the same spatial and/or temporal characteristics. The number of clusters in mmWaves is typically modeled by a Poisson distribution whose variance depends on the scenario and operating frequency. In the considered case, according to [42], the maximum number of clusters that can be chosen for the considered frequency (34.35 GHz) is 2. Here both cases with 1 and 2 clusters are taken into account. As regards the number of sub-rays, this number is usually an integer uniformly distributed between 1 and 30 for the adopted bandwidth [43]. For a sake of simplicity, we assume that the number of sub-rays is fixed to 5, 15 or 30. This assumption does not affect the quality of the results.

For each cluster, the azimuth departure angles $\phi_{c,s}^{TX}$

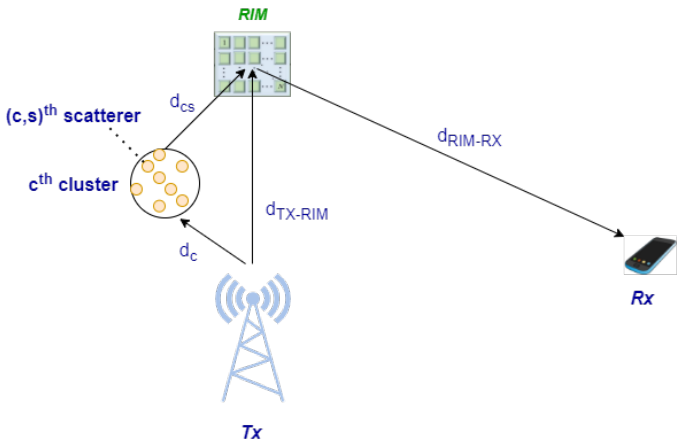

Figure 6. Channel model of a RIM-assisted system in presence of scatterers.

of the sub-rays are described by a Laplacian distribution whose mean value ϕ_c^{TX} is uniformly distributed $U[-\pi/2,\pi/2]$ and the standard deviation is $\sigma_\phi = 5°$[44]. Also the elevation departure angles $\theta_{c,s}^{TX}$ are conditionally Laplacian with the mean value θ_c^{TX} uniformly distributed $U[-\pi/4,\pi/4]$ and the standard deviation $\sigma_\theta = 5°$[45]. These departure angles are considered from the

transmitter side.
In order to simplify the next computations, all the scatterers belonging to a certain cluster are assumed to be at the same distance d_c from the transmitter. Moreover, d_c is assumed to be uniformly distributed between 1 and d_{TX-RIM}, where d_{TX-RIM} is the LOS link between the transmitter and the metasurface. The distance between each scatterer and the RIM is given by $d_{c,s}$. The distance between TX and RIM d_{TX-RIM} has been computed as:

$$d_{TX-RIM} = ((x^{RIM} - x^{TX})^2 + (y^{RIM} - y^{TX})^2 + (z^{RIM} - z^{TX})^2)^{1/2} \quad (10)$$

where (x^{RIM},y^{RIM},z^{RIM}) and (x^{TX},y^{TX},z^{TX}) are the coordinates of the RIM and of the TX respectively. From the TX coordinates, the coordinates of each scatterer of a cluster are computed by:

$$x_{c,s} = x^{TX} + a_c cos(\theta_{c,s}^{TX}) cos(\phi_{c,s}^{TX}) \quad (11)$$

$$y_{c,s} = y^{TX} - a_c cos(\theta_{c,s}^{TX}) sin(\phi_{c,s}^{TX}) \quad (12)$$

$$z_{c,s} = z^{TX} + a_c sin(\theta_{c,s}^{TX}) \quad (13)$$

The distance between each scatterer and the RIM is calculated as:

$$d_{c,s} = ((x^{RIM} - x^{c,s})^2 + (y^{RIM} - y^{c,s})^2 + (z^{RIM} - z^{c,s})^2)^{1/2} \quad (14)$$

Finally, the RIM arrival angles are obtained by:

$$\phi_{c,s}^{RIM} = I_\phi tan^{-1} \frac{|x^{RIM} - x^{c,s}|}{|y^{RIM} - y^{c,s}|} \quad (15)$$

with:

$$I_\phi = sgn(y^{c,s} - y^{RIM}) \quad (16)$$

$$\theta_{c,s}^{RIM} = I_\theta sin^{-1} \frac{|z^{RIM} - z^{c,s}|}{d_{c,s}} \quad (17)$$

where:

$$I_\theta = sgn(z^{c,s} - z^{RIM}) \quad (18)$$

From the RIM arrival angles $\theta_{c,s}^{RIM}$ of the signals reflected by the scatterers, that correspond to the incidence angle on the metasurface, the values of electric field reflected by the metasurface are evaluated. They have been computed also considering different values for the amplitude of the signals reflected by the scatterers, from 0.01V/m to 1V/m, where the last one corresponds to the value of the transmitted signal from the base station. These values have been combined with the electric field generated for the incidence of the signal transmitted by the base station. The value of the electric fields have been computed through this formula:

$$E = \sum_{ii=1}^{m} \sum_{jj=1}^{n} A_{\mathrm{mn}}\, e^{j\alpha_{\mathrm{mn}}}\, cos(\theta_{\mathrm{mn}})\, \|\Gamma_{\mathrm{ii,jj}}\|\, cos(tt)\, e^{i<\Gamma_{\mathrm{ii,jj}} + i\,k\,d\,\xi_{\mathrm{ii,jj}}} \quad (19)$$

$$with \quad \xi_{\mathrm{ii,jj}} = ((ii - \frac{1}{2})\cos(pp) + (jj - \frac{1}{2})\sin(pp))\sin(tt) \quad (20)$$

where m and n are the number of meta-atoms in the two dimensions, Γ is the reflection coefficient, k is the wavelength number and d is the distance among two adjacent meta-atoms (that corresponds to the length of a meta-atom, $3.81mm$ in this specific work). A_{mn} and α_{mn} are the amplitude and phase of the wave incident on the mn-th unit cell (set respectively to 1 and 0°), cos(θ,ϕ) is the scattering pattern of the mn-th unit cell (assuming meta-atoms as real-world dipolar scatterers), θ_{mn} corresponds to the incidence angle of the impinging signal that is measured from the perpendicular line to the metasurface. It has been set to 0°(orthogonal incidence) as regards the electric field component computed from the signal transmitted by the base station. tt and pp are two matrices made by the copy of two vectors θ and ϕ respectively in each row and in each column. More specifically, θ is a vector made by 100 equi-spaced values between 0 and $\frac{\pi}{2}$, while ϕ is made of the same number of values between 0 and 2π. The values of Γ are the ones evaluated for the meta-atom during the simulation.
Since the scatterers belonging to a cluster are very close to each other, the same arrival angle of the signals reflected by the scatterers of a cluster have been taken into account to make the computations faster, even though this assumption does not affect the global evaluation.

7 Performance evaluation

In this section the performance of the system consisting of a base station, our designed reconfigurable intelligent metasurface and a mobile receiver are evaluated in presence of interferers between the base station and the metasurface.

The phase configurations computation of the metasurface performing beam-steering is based on the PSO algorithm. This algorithm searches the phase configuration of the metasurface that allows to generate the radiation pattern with the direction of the main beam given in input to the algorithm. The maximum allowed S_{LL} has been set to 0.5 because the beam-width of the main beam is computed as HPBW (Half Power Beam-Width). In order to distinguish the main beam from the sidelobes, the sidelobe power should be lower than the half of the maximum power of the main beam.
Moreover, we have considered the interval of angles 200°-340°for the azimuth ϕ angle, while the elevation angle θ remains fixed to 12°. That interval has been

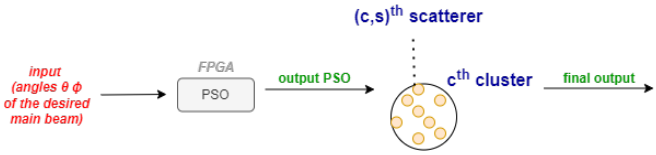

Figure 7. Scheme of the input and output of the PSO and of the output in presence of scatterers.

adopted for the azimuth angles because our aim is tracking a mobile user who walks on the street and by putting the reconfigurable intelligent metasurface over a building facade, all the other angles cannot be used for tracking (for example at 90 °of azimuth angle the main beam would be directed towards the sky, that is not useful for our purpose).
The maximum sidelobe level of the radiation pattern generated by the metasurface and the angular deviations δ_θ and δ_ϕ of the main beam of the obtained radiation pattern have been evaluated for four different directions of the main beam, 225°, 260°, 315°and 340°. We consider a single cluster of 5/15/30 scatterers whose scattered signals impinge on the metasurface at a fixed angle 30°/50°/85°(table 3).

Table 3.

angles of incidence	30°, 50°, 85°
number of scatterers	5, 15, 30
E field magnitudes of the scattered signals	0.1, 0.5

Also the case with two clusters have been evaluated whose scattered signals impinge on the metasurface with 30°and 50°respectively. Two different amplitudes of the electric field of the scattered signals 0.1V/m and 0.5V/m have been taken into account. The deviations δ_θ and δ_ϕ have been evaluated between the final output of the metasurface (in presence of scatterers) and the input of the PSO and between the final output of the metasurface and the output of the PSO. A scheme of the outputs is shown in Fig.7. As it is possible to notice from the fig. 8, the maximum SLL moves away from the case without scatterers when the power and the number of the scatterers increases. Moreover, the radiation patterns improve in terms of SLL when the angle of incidence is increased from 30°to 85°. This can be explained by the fact that at 30°phase shifts are a bit less close to 90°with respect to 50°. At 85°phases of S_{11} are completely different from the ones at 0°, so the impact of scatterers is low. Considering the case with two clusters, the SLL gets worse wrt. all the cases where one cluster is considered. For the main beam 340°the sidelobe level is lower than the other cases for any cluster configuration because the SLL of the radiation pattern at 340°without interference is very low compared to the other radiation patterns. Regarding the deviations of the angles of the main beam (fig.9,10, 11 and 12), they don't have a specific trend wrt. the number and the power of the scatterers because the chosen phase configurations from the algorithm seem to be insensitive in terms of direction of the generated main beam, that is a desired feature for our system.
The accuracy of the adopted algorithm to compute the best phase configuration has been evaluated through the computation of the confusion matrices. They allow to evaluate the errors in terms of direction of the beam made by the algorithm in presence of interferers. For the adopted meta-atom structure and the chosen algorithm, the accuracy is 85.71% for all the considered clusters configurations and for all the powers scattered by the interferers. This can be explained from the fact that the adopted metasurface generates radiation patterns robust against the interference (the radiation patterns are not distorted, only the SLL is increased) and the PSO is enough powerful not to provide wrong radiation patterns.

8 Tracking system for a mobile user

In this section we consider the case in which a mobile user needs to be tracked. We assume that the user walks at three different speeds, 6 km/h, 15 km/h and 35km/h, on a straight street. Our previously-discussed metasurface is adopted to perform the task. It is assumed also that there are no interferers between the base station and the RIM and between the RIM and the user.
The metasurface has the same dimension of the previous one (57.1 mm x 57.1 mm) and it covers the same path (282.8 meters) at a distance that varies from 200 meters (when the signal reflected from the metasurface has a main beam at ϕ= 225°and ϕ=-45°) and 141.4 meters (when the signal has a main beam at ϕ=270°).
Figure 13 shows the amount of time needed to cover a certain distance, according to different speeds of the user. The same times of the previous metasurface are required to cover a straight street of 282.8 meters (169.36 s in case of a pedestrian at 6 km/h, 67.83 s for a pedestrian at 15 km/h, 29.1 s for a person who rides a scooter at 35 km/h). As it is possible to notice from the graph, in this case four different beams (224.9°, 254.5°, 280°and -45°) are necessary in order to track a person over 282.8 meters. Table 4 shows all the time intervals, the distances and the angular distances covered for each speed of the user and for different directions of the main beams reflected by the metasurface. Increasing the speed of the user from 6 km/h to 35 km/h, the total time is reduced by 4 times. Further, in the table it is specified the change of the angular position of the user due to the computation time of the PSO. This change is very small, around 0.3°, and it has been checked that it does not have impact on the choice of the direction of the main beam reflected by the RIM.

9 Conclusions

In this paper, a new reconfigurable intelligent metasurface with beam-steering capabilities working at 34.35 GHz has been presented. First, the meta-atom structure has been designed in order to be reflective and to be insensitive to the angle of incidence until ± 75°. Particle Swarm Optimization (PSO) has been adopted to find the optimal phase configurations, both in terms of

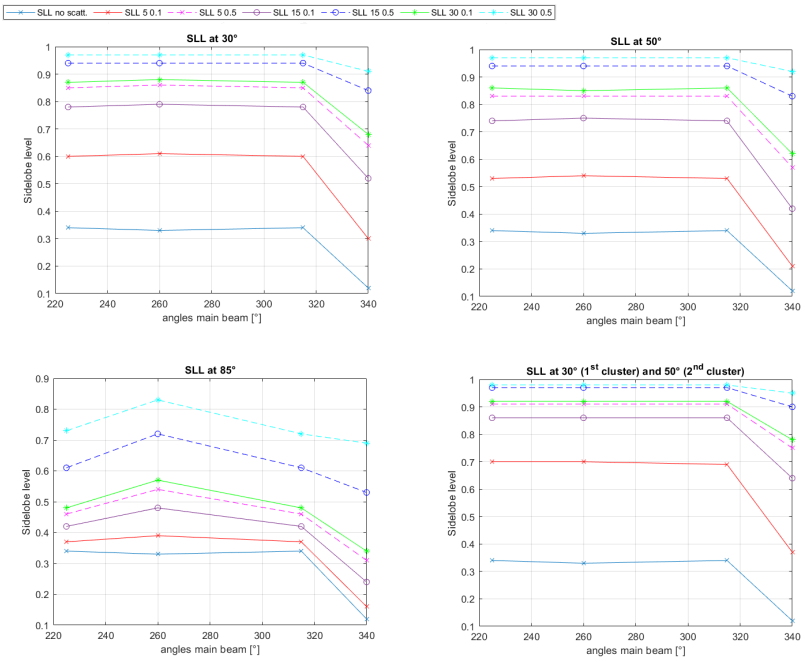

Figure 8. Sidelobe level for different angles of incidence of the signal reflected by one or two clusters.

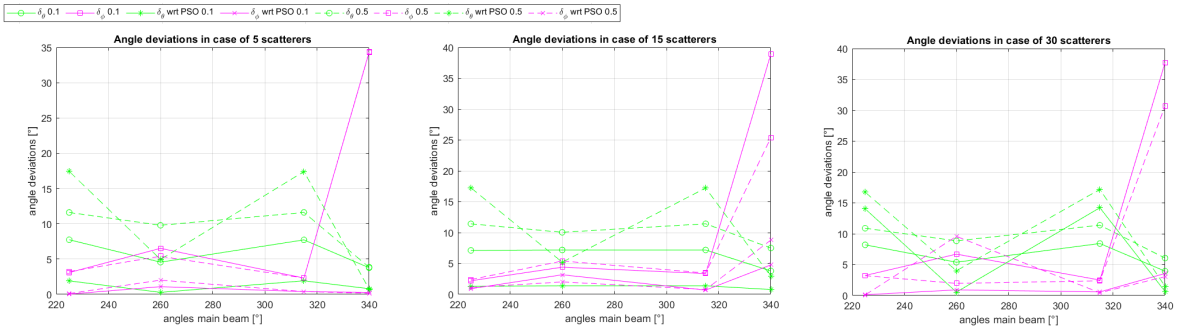

Figure 9. Angle deviations with 30°angle of incidence of the cluster of scatterers.

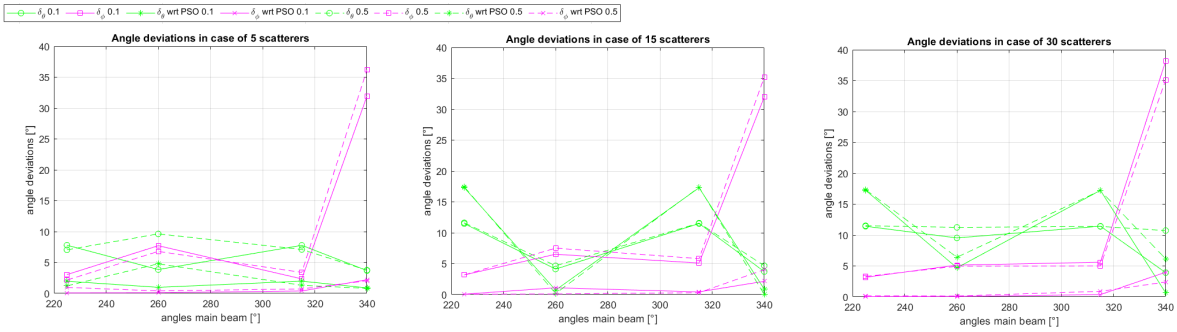

Figure 10. Angle deviations with 50°angle of incidence of the cluster of scatterers.

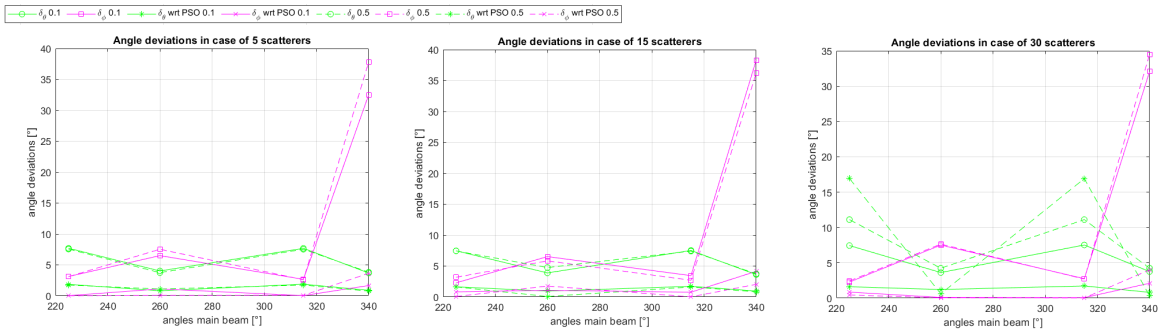

Figure 11. Angle deviations with 85°angle of incidence of the cluster of scatterers.

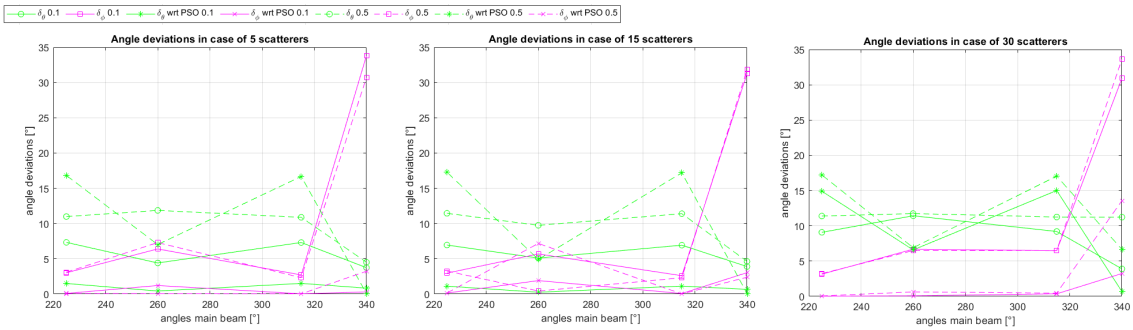

Figure 12. Angle deviations with two clusters, one at 30°and the other one at 50°angle of incidence.

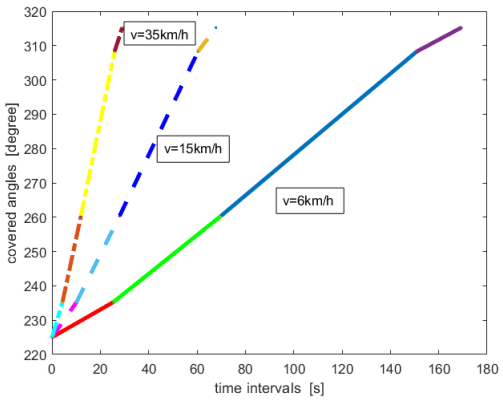

Figure 13. Time intervals in which the same beam can cover a certain angular distance, considering different speeds of the mobile user. Each coloured line stands for the beam adopted to cover a given distance during a certain time interval.

phase and side lobe levels, of the metasurface to perform beam-steering. Then a realistic wireless system in outdoor environment has been evaluated in presence of interferers between the transmitter and the RIM. Performances of PSO algorithm in presence of 5/15/30 scatterers have been evaluated in terms of deviations of the obtained main beam from the desired one, obtained sidelobe level and accuracy of the algorithm. The deviations of the angles of the main beam don't have a specific trend wrt. the number and the power of the scatterers because the chosen phase configurations from the algorithm is insensitive in terms of direction of the generated main beam. Besides, the maximum SLL increases when the power and the number of the scatterers increase. As regards its behaviour wrt. the angle of incidence of the scatterers, it depends on the radiation pattern: in case of 260°and -20°SLL gets worse when the angle of incidence is increased; in case of 225°and 315°, the behaviour improves from 30°to 85°. This can be explained by the fact that at 30°phase shifts are a bit less close to 90°with respect to 50°. At 85°phases of S_{11} are completely different from the ones at 0°, so the impact of scatterers is low. As regards the accuracy, it is 85.71% for all the considered clusters configurations because even in presence of scatterers main beams are never distorted or reduced in width. Finally, a tracking system is considered where the designed metasurface is adopted to track a mobile receiver on a path of 282.8 meters at three different speeds: 6 km/h, 15 km/h and 35km/h. Four different radiation patterns are required to maintain the tracking. Moreover, during the change

Table 4. Results

v [km/h]	adopted beam	t [s]	d [m]	ϕ	$\phi_{afterGA}$
6	224.9°	0 - 25.39	0 - 42.4	225°- 235°	225.25°- 235.25°
6	254.5°	25.39 - 69.88	42.4 - 116.7	235°-260°	235.25°-260.34°
6	280°	69.88 - 150.9	116.7 - 252	260°-308°	260.34°-308.28°
6	315°	150.9 - 169.36	252 - 282.84	308°-315°	308.28°-315.25°
15	224.9°	0 - 10.17	0 - 42.4	225°-235°	225.25°- 235.25°
15	254.5°	10.17 - 27.98	42.4 - 116.7	235°-260°	235.25°-260.34°
15	280°	27.98 - 60.43	116.7 - 252	260°-308°	260.34°-308.28°
15	315°	60.43 - 67.83	252 - 282.84	308°-315°	308.28°-315.25°
35	224.9°	0 - 4.36	0 - 42.4	225°-235°	225.25°- 235.25°
35	254.5°	4.36 - 12	42.4 - 116.7	235°-260°	235.25°-260.34°
35	280°	12 - 25.92	116.7 - 252	260°-308°	260.34°-308.28°
35	315°	25.92 - 29.1	252 - 282.84	308°-315°	308.28°-315.25°

of the phase configuration of the metasurface, no loss of tracking occurs.

10 Acknowledgments

This work has been partially supported by the Horizon Europe MLSysOps project, DOI 10.3030/101092912.

11 References

[1] C. Liaskos, S. Nie, A. Tsioliaridou, A. Pitsillides, S. Ioannidis and I. Akyildiz, "A New Wireless Communication Paradigm through Software-Controlled Metasurfaces," in IEEE Communications Magazine, vol. 56, no. 9, pp. 162-169, Sept. 2018, doi: 10.1109/MCOM.2018.1700659.

[2] Renzo, M.D., Debbah, M., Phan-Huy, DT. et al. Smart radio environments empowered by reconfigurable AI meta-surfaces: an idea whose time has come. J Wireless Com Network 2019, 129 (2019). https://doi.org/10.1186/s13638-019-1438-9

[3] E. Basar, M. Di Renzo, J. De Rosny, M. Debbah, M. -S. Alouini and R. Zhang, "Wireless Communications Through Reconfigurable Intelligent Surfaces," in IEEE Access, vol. 7, pp. 116753-116773, 2019, doi: 10.1109/ACCESS.2019.2935192.

[4] W. Tang et al., "Wireless Communications With Reconfigurable Intelligent Surface: Path Loss Modeling and Experimental Measurement," in IEEE Transactions on Wireless Communications, vol. 20, no. 1, pp. 421-439, Jan. 2021, doi: 10.1109/TWC.2020.3024887.

[5] W. Chen, L. Bai, W. Tang, S. Jin, T. Cui, "Angle-Dependent Phase Shifter Model for Reconfigurable Intelligent Surfaces: Does the Angle- Reciprocity Hold?" IEEE Communications Letters, PP.99(2020):1-1.

[6] J. C. Liang et al., "An Angle-Insensitive 3-Bit Reconfigurable Intelligent Surface," in IEEE Transactions on Antennas and Propagation, doi: 10.1109/TAP.2021.3130108.

[7] L. Zhang and T. J. Cui, "Angle-Insensitive 2-Bit Programmable Coding Metasurface with Wide Incident Angles," 2019 IEEE Asia-Pacific Microwave Conference (APMC), 2019, pp. 932-934, doi: 10.1109/APMC46564.2019.9038764.

[8] M. Di Renzo et al., "Reconfigurable Intelligent Surfaces vs. Relaying: Differences, Similarities, and Performance Comparison," in IEEE Open Journal of the Communications Society, vol. 1, pp. 798-807, 2020, doi: 10.1109/OJCOMS.2020.3002955.

[9] R. Mehrotra et al., "3D Channel Modeling and Characterization for Hypersurface Empowered Indoor Environment at 60 GHz Millimeter-Wave Band," 2019 International Symposium on Performance Evaluation of Computer and Telecommunication Systems (SPECTS), 2019, pp. 1-6, doi: 10.23919/SPECTS.2019.8823296.

[10] H. Taghvaee et al., "Scalability Analysis of Programmable Metasurfaces for Beam Steering," in IEEE Access, 2020.

[11] Huang, Cheng et al.,"Dynamical beam manipulation based on 2-bit digitally-controlled coding metasurface," Scientific reports vol. 7, 2017.

[12] Wan, X., Qi, M., Chen, T. et al. Field-programmable beam reconfiguring based on digitally-controlled coding metasurface. Sci Rep 6, 2016.

[13] V. Asadchy, M. Albooyeh, S. N. Tcvetkova, A. D'iaz-Rubio, Y Ra'di and Sergei A. Tretyakov, "Perfect control of reflection and refraction using spatially dispersive metasurfaces", Physical Review B, 2016.

[14] J. C. Liang et al., "An Angle-Insensitive 3-Bit Reconfigurable Intelligent Surface," in IEEE Transactions on Antennas and Propagation, 2021.

[15] L. Zhang and T. J. Cui, "Angle-Insensitive 2-Bit Programmable Coding Metasurface with Wide Incident Angles," 2019 IEEE Asia-Pacific Microwave Conference (APMC), 2019.

[16] Hashemi, M., Yang, SH., Wang, T. et al,"Electronically-Controlled Beam-Steering through Vanadium Dioxide Metasurfaces",Sci Rep 6, 35439, https://doi.org/10.1038/srep35439, 2016.

[17] Hashemi, Mohammed Reza M. and Yang, Shang-Hua and Wang, Tongyu and Sepúlveda, Nelson and Jarrahi, Mona, "Reconfigurable meta-surface for millimeter-wave beam-scanning", 41st International Conference on Infrared, Millimeter, and Terahertz waves (IRMMW-THz), 2016.

[18] Hashemi, Mohammed Reza M. and Yang, Shang-Hua and Wang, Tongyu and Sepúlveda, Nelson and Jarrahi, Mona, "Fully-integrated and electronically-controlled millimeter-wave beam-scanning", IEEE MTT-S International Microwave Symposium (IMS), 2016.

[19] Vassos, E., Churm, J., Powell, J. et al., Air-bridged Schottky diodes for dynamically tunable millimeter-wave metamaterial phase shifters, Sci Rep 11, 5988, https://doi.org/10.1038/s41598-021-85565-z, 2021.

[20] Yin, Jiexi and Wu, Qi and Lou, Qun and Wang, Haiming and Chen, Zhi Ning and Hong, Wei, "Single-Beam 1 Bit Reflective Metasurface Using Prephased Unit Cells for Normally Incident Plane Waves", IEEE Transactions on Antennas and Propagation, 2020.

[21] Cho, Kun Woo and Mazaheri, Mohammad H. and Gummeson, Jeremy and Abari, Omid and Jamieson, Kyle, "MmWall: A Reconfigurable Metamaterial Surface for MmWave Networks", https://doi.org/10.1145/3446382.3448665, 2021.

[22] Feng, Chao and Zhang, Yangfan and Wang, Xiaojing and Li, Xinyi, "A Low-Cost and Reconfigurable Metasurface for MmWave Networks: Poster Abstract", https://doi.org/10.1145/3498361.3538770, 2022.

[23] J. C. Liang et al., "An Angle-Insensitive 3-Bit Reconfigurable Intelligent Surface," in IEEE Transactions on Antennas and Propagation, 2021.

[24] L. Zhang and T. J. Cui, "Angle-Insensitive 2-Bit Programmable Coding Metasurface with Wide Incident Angles," 2019 IEEE Asia-Pacific Microwave Conference (APMC), 2019.

[25] W. Tang et al.,"Wireless communications with reconfigurable intelligent surface: Path loss modeling and experimen-

tal measurement",https://arxiv.org/abs/1911.05326, 2019.
[26] V. Jamali, A. M. Tulino, G. Fischer, R. Mller, and R. Schober, "Intelligent reflecting and transmitting surface aided millimeter wave massive MIMO", https://arxiv.org/abs/1902.07670, 2019.
[27] M. Jian et al.,"Reconfigurable intelligent surfaces for wireless communications: Overview of hardware designs, channel models, and estimation techniques",Intelligent and Converged Networks, vol. 3, no. 1, pp. 1-32,2022.
[28] R. Zhou, X. Chen, W. Tang, X. Li, S. Jin, E. Basar, Q. Cheng, and T. J. Cui ,"Modeling and measurements for multi-path mitigation with reconfigurable intelligent surfaces", https://arxiv.org/pdf/2109.11820, 2021.
[29] E. Basar, I. Yildirim, and F. Kilinc ,"Indoor and outdoor physical channel modeling and efficient positioning for reconfigurable intelligent surfaces in mmWave bands", IEEE Trans. Commun., vol. 69, no. 12, pp. 8600–8611, 2021.
[30] Liaskos, Christos and Nie, Shuai and Tsioliaridou, Ageliki and Pitsillides, Andreas and Ioannidis, Sotiris and Akyildiz, Ian,"Realizing Wireless Communication through Software-defined HyperSurface Environments", https://arxiv.org/abs/1805.06677, 2018.
[31] R. Mehrotra et al.,"3D Channel Modeling and Characterization for Hypersurface Empowered Indoor Environment at 60 GHz Millimeter-Wave Band", International Symposium on Performance Evaluation of Computer and Telecommunication Systems (SPECTS), 2019.
[32] Joonas Kokkoniemi and Markku J. Juntti,"Channel modeling for reflective phased array type RISs in mmWave networks",Proceedings of the 5th ACM Workshop on Millimeter-Wave and Terahertz Networks and Sensing Systems, 2021.
[33] Carola Rizza and Valeria Loscri, "Study on the Interference of a Communication System based on a Meta-surface in mmWave", accepted at IEEE GLOBECOM 2022.
[34] Wan Jiang, Yong Mao Huang, Biao Zhang, Jianhang Ling and Christian Waldschmidt,"A Ka-band pattern-reconfigurable microstrip antenna enabled by PIN diodes with accurate extraction of equivalent circuit parameters,"Journal of Physics D: Applied Physics, 2021.
[35] Sensong An, Bowen Zheng, Mikhail Y. Shalaginov, Hong Tang, Hang Li, Li Zhou, Jun Ding, Anuradha Murthy Agarwal, Clara Rivero-Baleine, Myungkoo Kang, Kathleen A. Richardson, Tian Gu, Juejun Hu, Clayton Fowler, and Hualiang Zhang, "Deep learning modeling approach for metasurfaces with high degrees of freedom," Opt. Express 28, 31932-31942 (2020).
[36] An, Sensong and Fowler, Clayton and Zheng, Bowen and Shalaginov, Mikhail Y. and Tang, Hong and Li, Hang and Zhou, Li and Ding, Jun and Agarwal, Anuradha Murthy and Rivero-Baleine, Clara and Richardson, Kathleen A. and Gu, Tian and Hu, Juejun and Zhang, Hualiang, "A Novel Modeling Approach for All-Dielectric Metasurfaces Using Deep Neural Networks", https://arxiv.org/abs/1906.03387, 2019.
[37] Computer Simulation Technology,
[38] Sawyer D. Campbell, David Sell, Ronald P. Jenkins, Eric B. Whiting, Jonathan A. Fan, and Douglas H. Werner, "Review of numerical optimization techniques for meta-device design [Invited]," Opt. Mater. Express 9, 1842-1863 (2019)
[39] Kennedy J, Eberhart RC. Particle swarm optimization. In: Proceedings of the International Conference on Neural Networks; Institute of Electrical and Electronics Engineers. Vol. 4. 1995. pp. 1942-1948.
[40] Yudong Zhang, Shuihua Wang, Genlin Ji, "A Comprehensive Survey on Particle Swarm Optimization Algorithm and Its Applications", Mathematical Problems in Engineering, vol. 2015.
[41] Bruno Seixas Gomes de Almeida and Victor Coppo Leite (December 3rd 2019). Particle Swarm Optimization: A Powerful Technique for Solving Engineering Problems, Swarm Intelligence - Recent Advances, New Perspectives and Applications, Javier Del Ser, Esther Villar and Eneko Osaba, IntechOpen, DOI: 10.5772/intechopen.89633. Available from: https://www.intechopen.com/books/swarm-intelligence-recent-advances-new-perspectives-and-applications/particle-swarm-optimization-a-powerful-technique-for-solving-engineering-problems
[42] I. A. Hemadeh, K. Satyanarayana, M. El-Hajjar and L. Hanzo, "Millimeter-Wave Communications: Physical Channel Models, Design Considerations, Antenna Constructions, and Link-Budget," in IEEE Communications Surveys & Tutorials, vol. 20, no. 2, pp. 870-913,2017.
[43] M. K. Samimi and T. S. Rappaport, "Statistical channel model with multi-frequency and arbitrary antenna beamwidth for millimeter-wave outdoor communications," in 2015 IEEE Globecom Workshops (GC Wkshps), 2015, pp. 1–7.
[44] S. Buzzi and C. D'Andrea, "On clustered statistical MIMO millimeter wave channel simulation," Apr. 2016. [Online]. Available: arXiv:1604.00648
[45] O. E. Ayach, S. Rajagopal, S. Abu-Surra, Z. Pi, and R. W. Heath, "Spatially sparse precoding in millimeter wave MIMO systems," IEEE Trans. Wireless Commun., vol. 13, no. 3, pp. 1499–1513, Mar. 2014.